Supporting Information

Bulk and transparent supramolecular glass from evaporation-induced noncovalent polymerization of nucleosides

Shuanggen Wu,[a,b] Changyong Cai,[a] Xunqiu Wang,[b] Qiao Zhang,[a] Zhijian Tan,*[c] Fenfang Li [d] and Shengyi Dong *[a]

[a]College of Chemistry and Chemical Engineering, Hunan University, Changsha 410082, Hunan, P. R. China.

[b]School of Chemical Engineering, Zhengzhou University, Zhengzhou 450001, Henan, P. R. China.

[c]Institute of Bast Fiber Crops, Chinese Academy of Agricultural Sciences, Changsha 410205, Hunan, P. R. China.

[d]College of Chemistry and Chemical Engineering, Central South University, Changsha 410083, Hunan, P. R. China.

*Corresponding author. E-mail: tanzhijian@caas.cn; dongsy@hnu.edu.cn

Table of Content

1. Contact angle measurements of BSGs

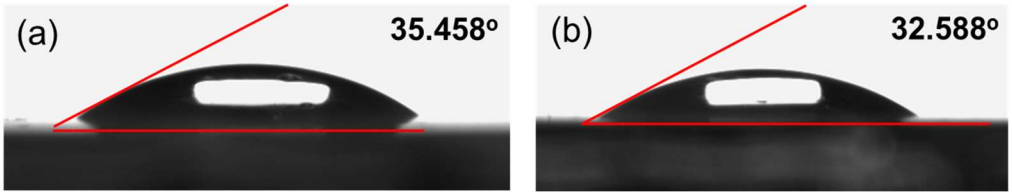

Figure S1. Contact angles of **BSG**s with water. The contact angles of (a) **UD** and (b) **TD**.

2. Optical microscope measurements of BSGs

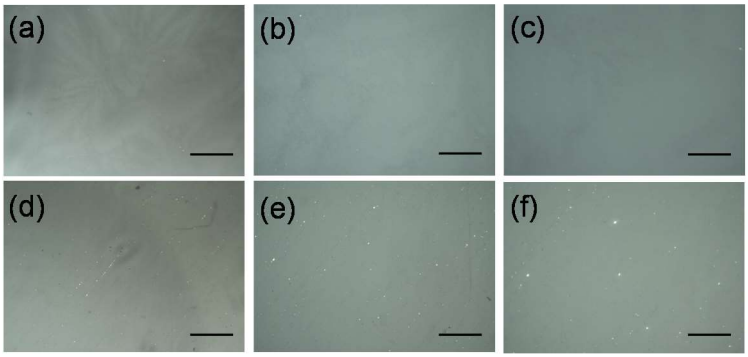

Figure S2. Optical microscope images of **BSG**s. (a–c) **TD**. (d–e) **UD**. Scale bar represent 20, 10, and 5 μm from left to right, respectively.

3. Atomic force microscopy (AFM) of BSGs

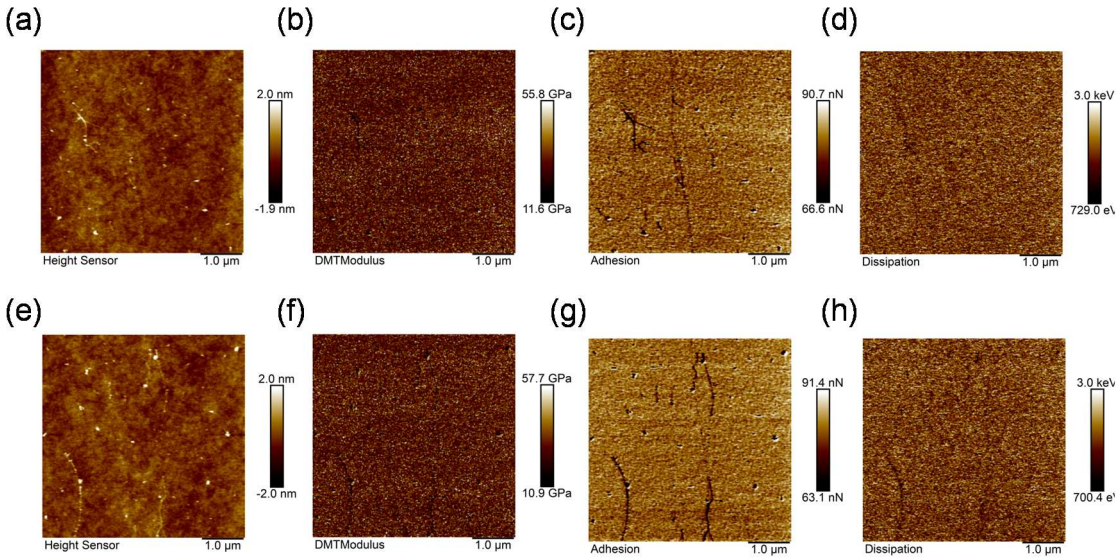

Figure S3. AFM phase images of **TD**.

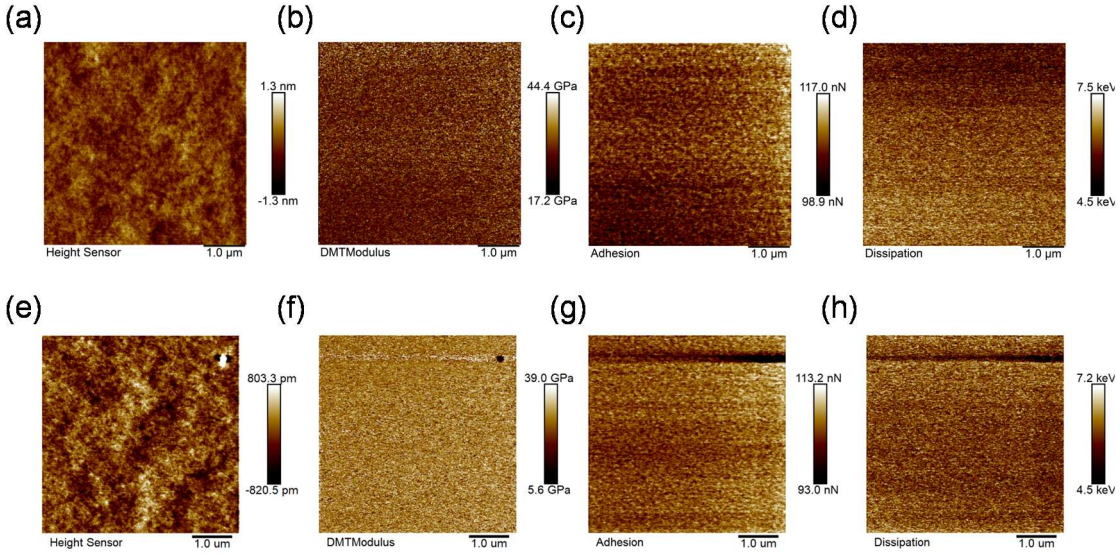

Figure S4. AFM phase images of **UD**.

4. Nanoindentation testing of BSGs

Table S1. Elastic modulus and hardness of **BSG**s.

BSGs	Elastic modulus (GPa)	Hardness (GPa)
TD	5.87 ± 0.47	0.0613 ± 0.0042
UD	4.50 ± 0.49	0.0258 ± 0.011

These data were obtained from nanoindentation tests.

5. Dynamic thermomechanical analysis (DMA) of BSGs

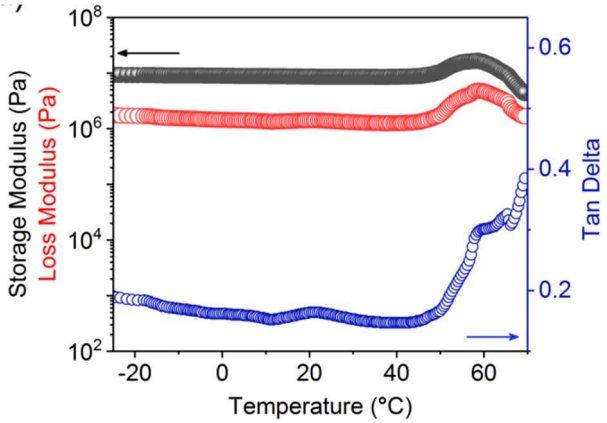

Figure S5. Temperature-dependent storage modulus, loss modulus, and tan δ of **TD**.

Table S2. Elastic modulus of **BSG**s obtained from different tests.

Supramolecular glass	Elastic modulus		
	Tensile test	Compression test	Nanoindentation test
TD	4.94 ± 0.32 MPa	58.7 ± 3.11 MPa	5.87 ± 0.47 GPa
UD	4.19 ± 0.11 MPa	34.6 ± 2.42 MPa	4.50 ± 0.49 GPa

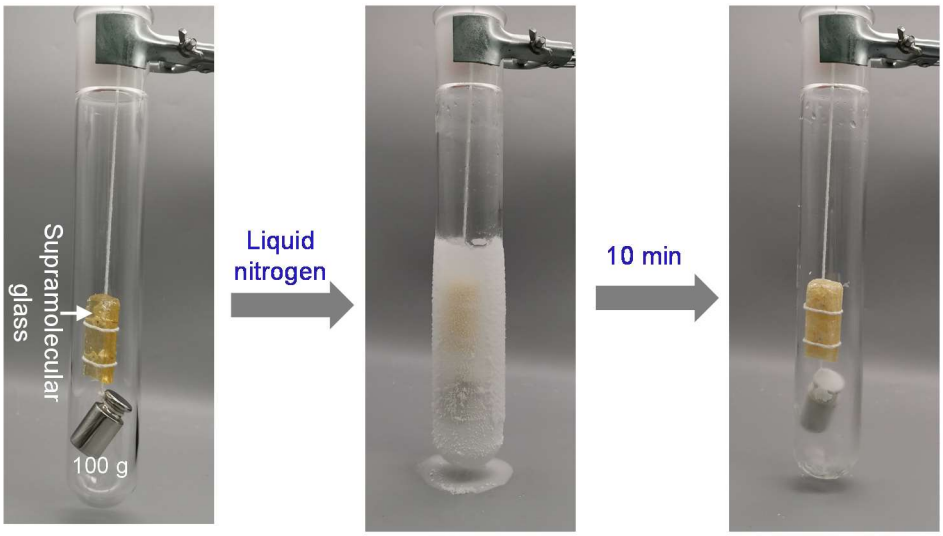

Figure S6. Macroscopic stretching behavior of **TD** in liquid nitrogen (50 × 25 × 10 mm^3).

6. Long-term stability of BSGs

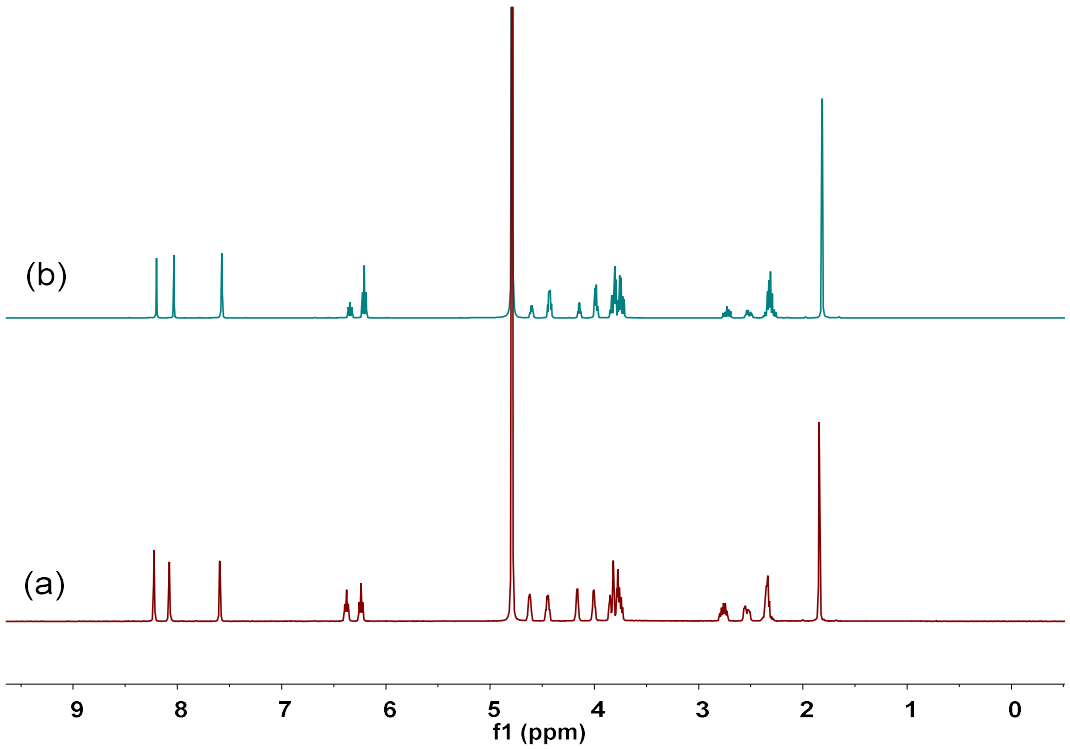

Figure S7. Time-dependent ^1H NMR spectra (400 MHz, D_2O, room temperature) of **TD**: (a) 0 day, (b) 30 days.

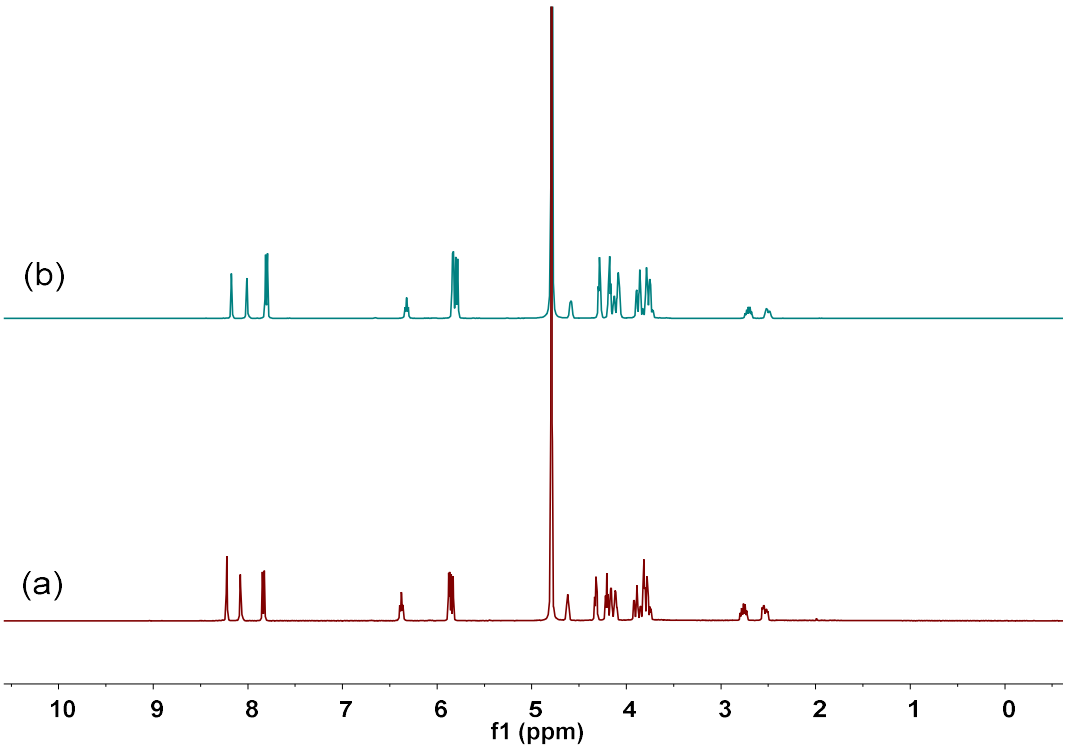

Figure S8. Time-dependent ^{1}H NMR spectra (400 MHz, D_2O, room temperature) of **UD**: (a) 0 day, (b) 30 days.

No obvious changes in ^{1}H NMR spectra of **BSG**s were observed after 30 days, suggesting that **BSG**s have excellent structural stability.

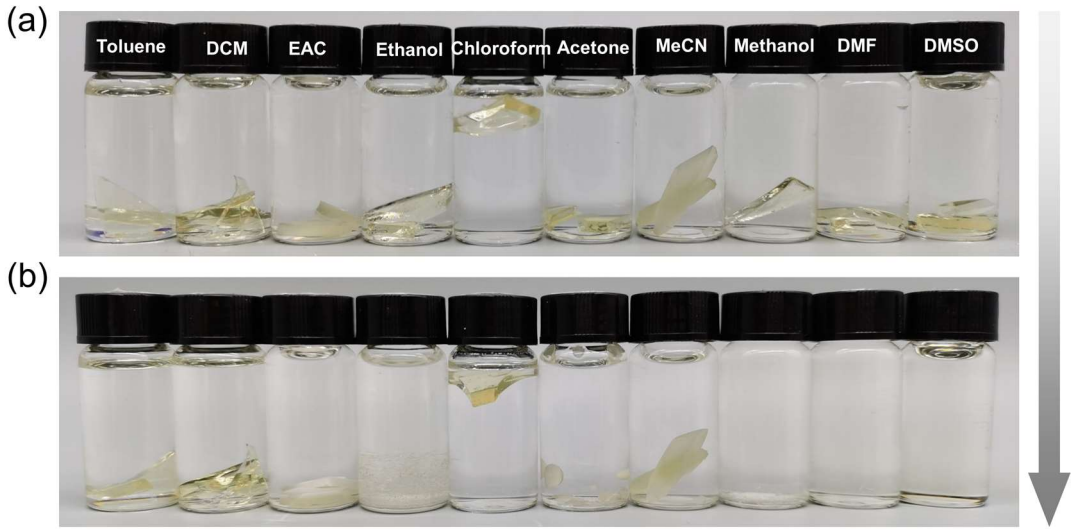

Figure S9. Time-dependent of **TD** soaked in different organic solvents: (a) 0 h; (b) 14 days. DCM, EAC, MeCN, DMF, DMSO represent dichloromethane, ethyl acetate, acetonitrile, N,N-dimethylformamide, dimethyl sulfoxide, respectively. DCM and EAC represent dichloromethane and ethyl acetate, respectively.

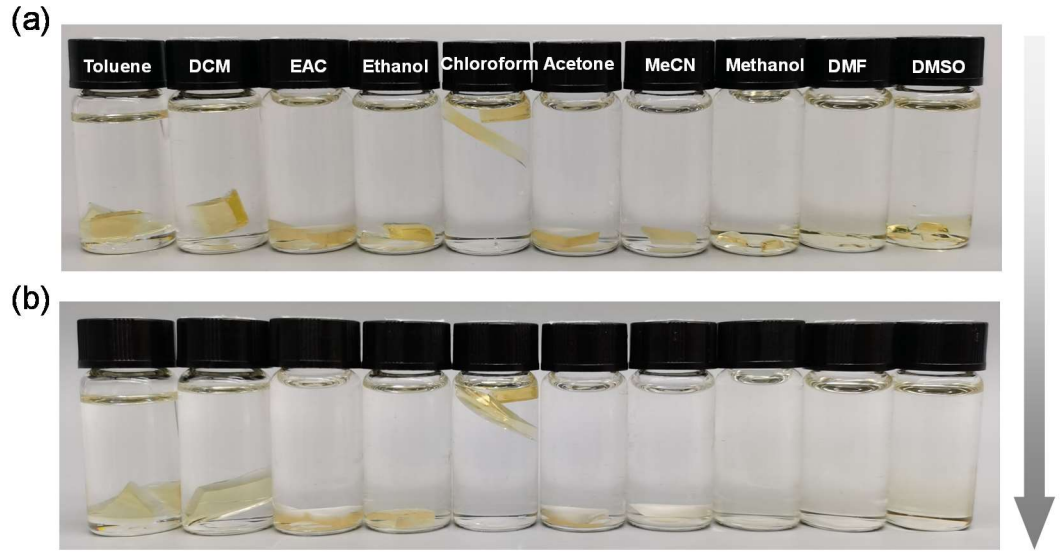

Figure S10. Time-dependent of **UD** soaked in different organic solvents: (a) 0 h; (b) 14 days. DCM, EAC, MeCN, DMF, DMSO represent dichloromethane, ethyl acetate, acetonitrile, N,N-dimethylformamide, dimethyl sulfoxide, respectively. DCM and EAC represent dichloromethane and ethyl acetate, respectively.

Table S3. Time-dependent transmittance of **TD** soaked in different organic solvents.

Time	Relative transmittance (%)						
(h)	Toluene	DCM	EAC	Ethanol	Chloroform	Acetone	Acetonitrile
0	100	100	100	100	100	100	100
5	96.4	99.1	8.5	6.9	96.1	3.4	3.0
24	95.4	95.2	7.1	6.6	95.5	2.3	2.6
168	93.2	93.4	6.9	5.4	94.4	0.8	2.4

DCM and EAC represent dichloromethane and ethyl acetate, respectively.

Table S4. Time-dependent transmittance of **UD** soaked in different organic solvents.

Time	Relative transmittance (%)						
(h)	Toluene	DCM	EAC	Ethanol	Chloroform	Acetone	Acetonitrile
0	100	100	100	100	100	100	100
5	96.8	97.7	3.9	3.0	98.9	4.3	4.9
24	96.6	97.6	2.1	2.5	95.5	3.9	4.6
168	91.5	90.4	1.8	2.2	94.8	2.6	4.0

DCM and EAC represent dichloromethane and ethyl acetate, respectively.

The stability of **BSG**s was evaluated in different organic solvents, including toluene, dichloromethane, ethyl acetate, ethanol, chloroform, acetone, acetonitrile, methanol, N,N-dimethylformamide, and dimethyl sulfoxide. **BSG**s can be dissolved in methanol, N,N-dimethylformamide, and dimethyl sulfoxide. The phase separations of **BSG**s were observed in ethyl acetate, ethanol, acetone, and acetonitrile. No obvious changes in transmittance of **BSG**s were observed in toluene, dichloromethane, and chloroform. These results show that **BSG**s exhibit good transmittance in low-polarity solvents. Meanwhile, after storing at 30% RH for7 days,

BSGs still displayed high values of transmittance (> 85%).

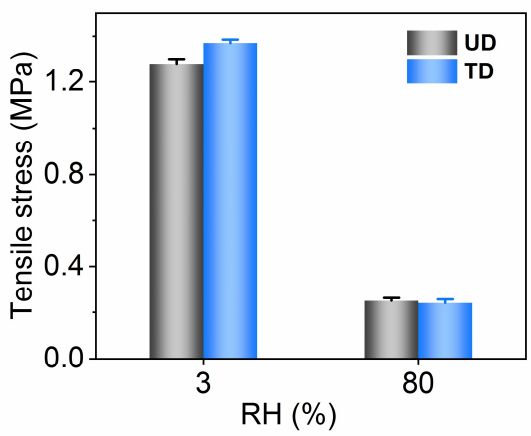

Figure S11. Relative humidity-dependent tensile stress of **UD** and **TD**.

Table S5. Time-dependent hardness of **TD** at different humidities.

Time (h)	Shore hardness (HD)		
	5% RH	30% RH	80% RH
24	31 ± 1	29 ± 2	2.1 ± 1
168	30 ± 3	30 ± 1	1.8 ± 3

The freshly prepared **TD** has the HD at 32 ± 2.

Table S6. Time-dependent hardness of **UD** at different humidities.

Time (h)	Shore hardness (HD)		
	5% RH	30% RH	80% RH
24	34 ± 1	28 ± 1	4.1 ± 1
168	32 ± 1	28 ± 2	1.2 ± 3

The freshly prepared **UD** has the HD at 36 ± 3.

The mechanical properties of **BSG**s were measured at different relative humidity (RH). Good tensile strength and high hardness of **TD** and **UD** were found under at 3% and 30% RH for 7 days (Fig. S11 and Table S5,6), indicating that the mechanical

performances of **BSG**s are stable at low-humidity environment. In contrast, **BSG**s exhibit poor mechanical properties at high-humidity environment (80% RH). A possible explanation is that a large amount of water molecules absorbed from the high-moisture environment can destroy inter-chain hydrogen bonds and induce the phase separation.

7. Rheology measurements of BSGs

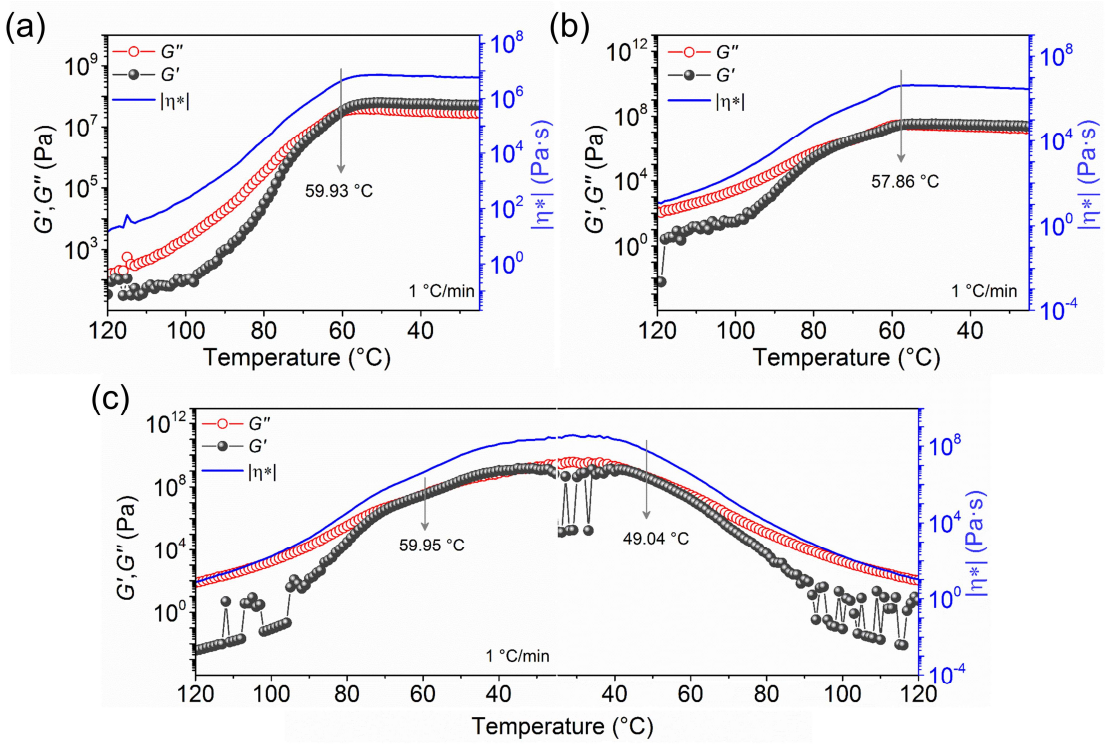

Figure S12. Rheological tests of **BSG**s. (a) Storage modulus (*G'*), loss modulus (*G''*), and composite viscosity (|η*|) values of **TD** at 1.0 ºC/min. (b) *G'*, *G''*, and |η*| value of **UD** at 1.0 ºC/min. (c) *G'*, *G''*, and |η*| value of **TD** at reversible temperature-dependent rheological tests.

8. ^{1}H NMR spectra of BSGs

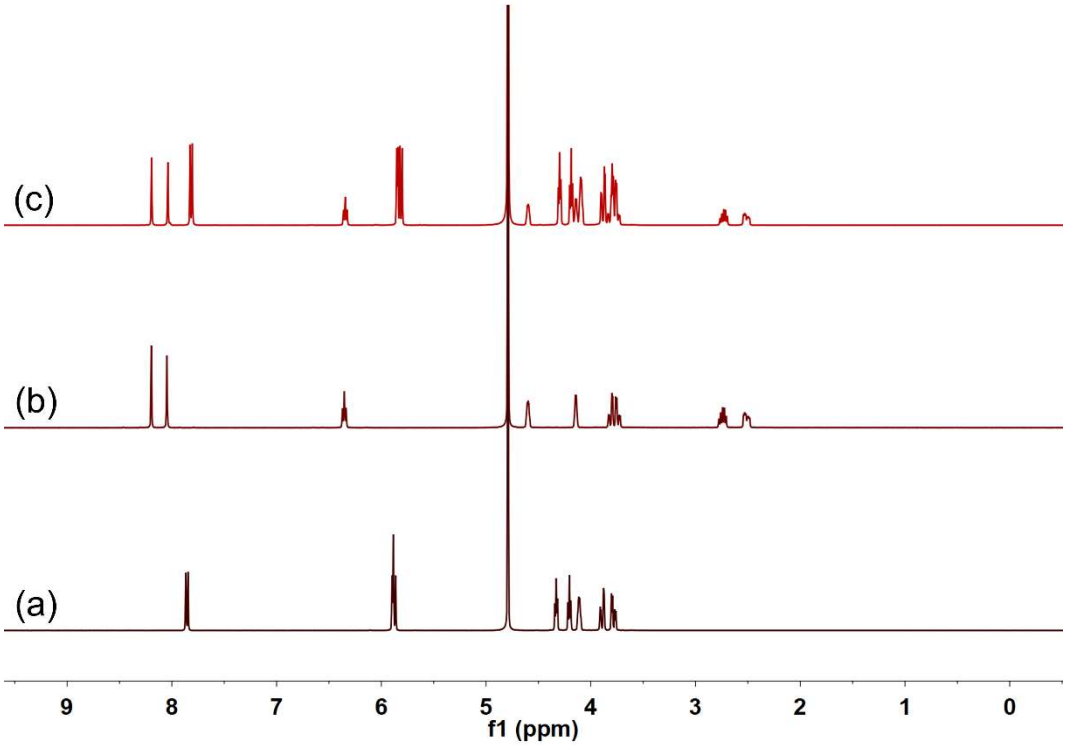

Figure S13. ^{1}H NMR spectra (400 MHz, D_2O, room temperature). (a) **U**. (b) **D**. (c) **UD**.

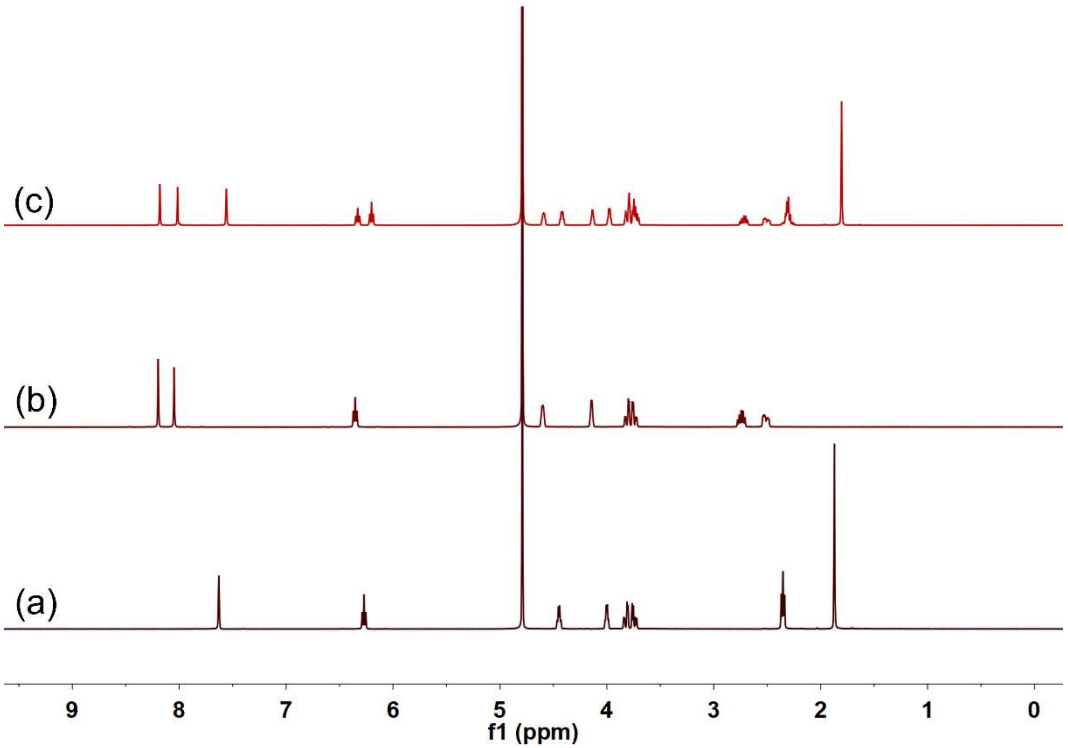

Figure S14. ^{1}H NMR spectra (400 MHz, D_2O, room temperature). (a) **T**. (b) **D**. (c)

TD.

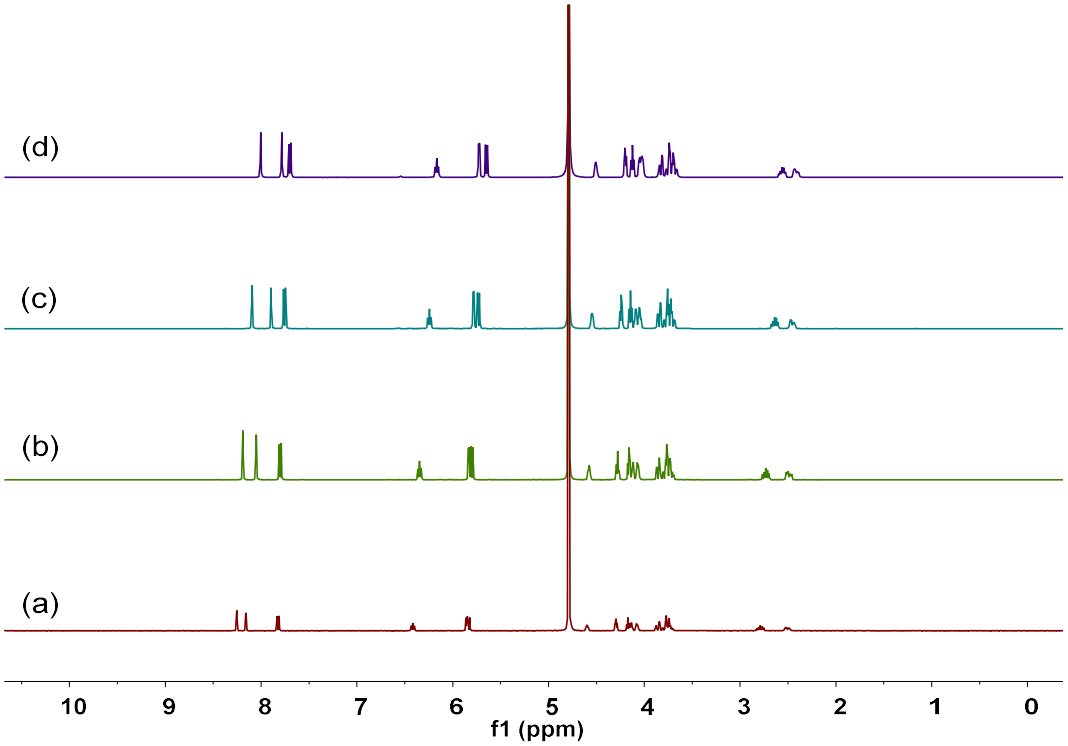

Figure S15. Concentration-dependent ^{1}H NMR spectra (400 MHz, D_2O, room temperature) of **UD**. (a) 4.0 mg/mL. (b) 20 mg/mL. (c) 100 mg/mL. (d) 300 mg/mL.

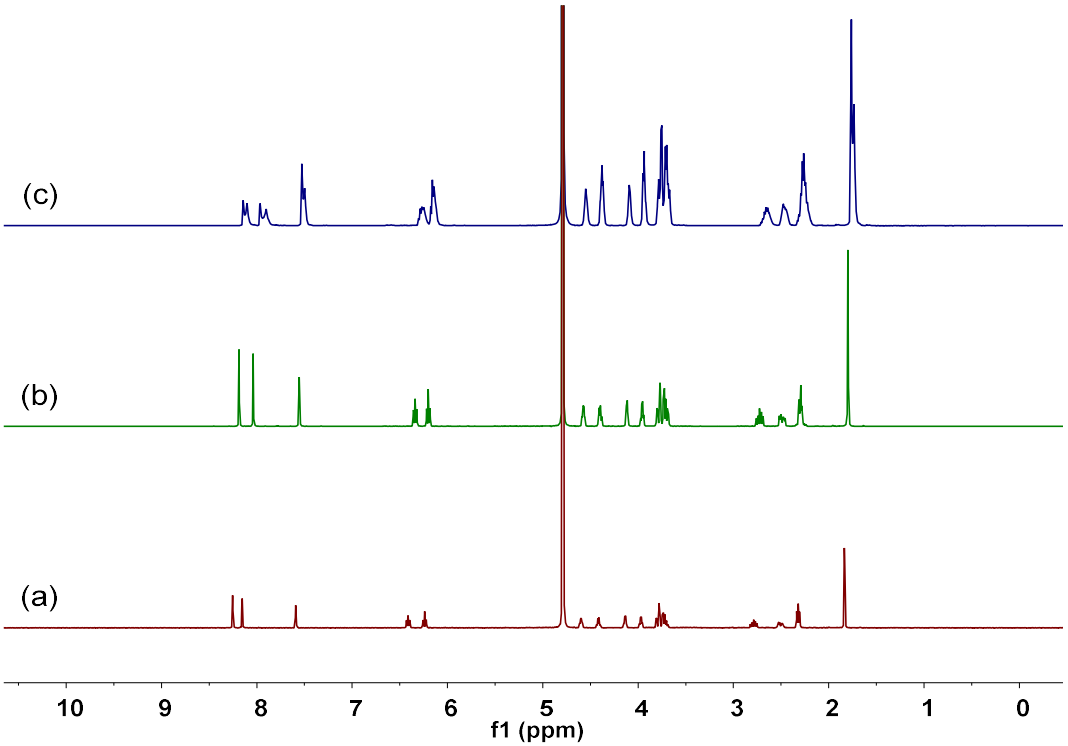

Figure S16. Concentration-dependent ^{1}H NMR spectra (400 MHz, D_2O, room temperature) of **TD**. (a) 4.0 mg/mL. (b) 20 mg/mL. (c) 100 mg/mL.

9. Raman spectra of BSGs

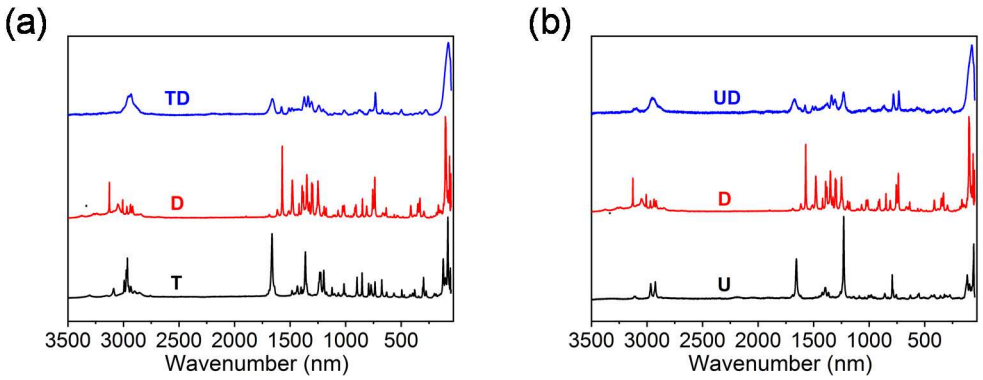

Figure S17. Raman spectra of nucleosides and **BSG**s. (a) Raman spectra of **T**, **D**, and **TD**. (b) Raman spectra of **U**, **D**, and **UD**.

10. Fourier-Transform infrared (FT-IR) spectra of BSGs

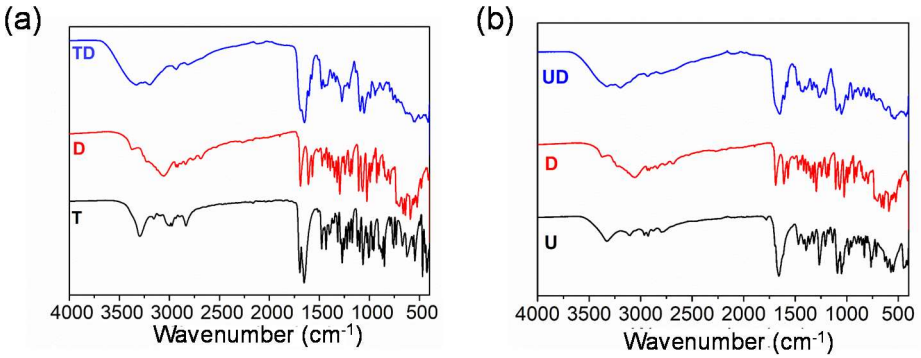

Figure S18. FT-IR spectra of nucleosides and **BSG**s. (a) FT-IR spectra of **T**, **D**, and **TD**. (b) FT-IR spectra of **U**, **D**, and **UD**.

11. Two-dimensional infrared correlation spectra of BSGs

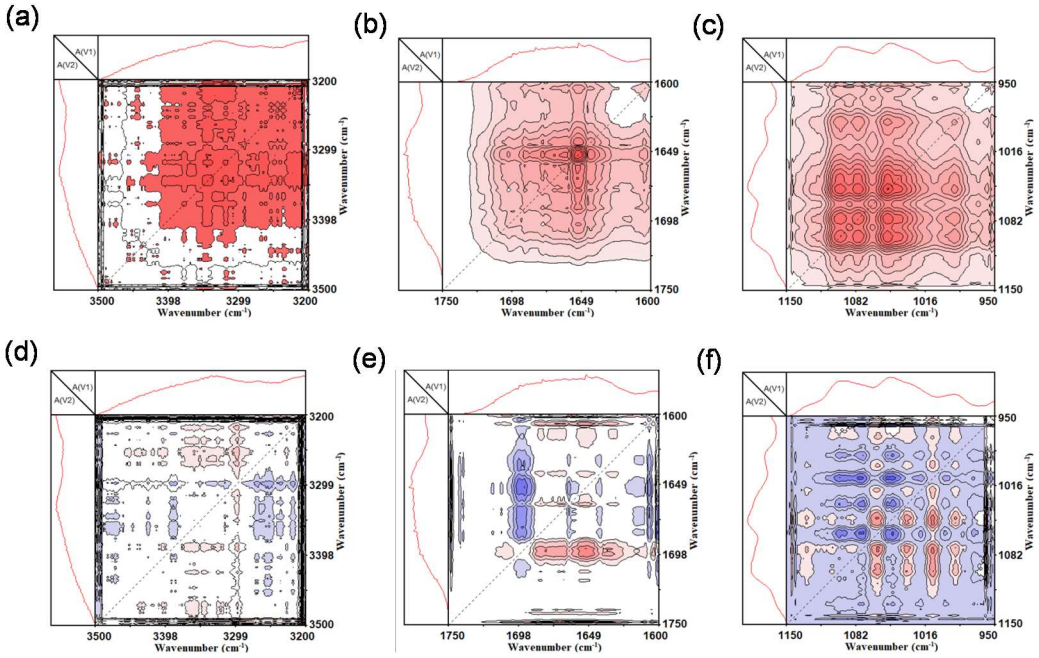

Figure S19. Synchronous and asynchronous correlation spectra of **TD** during heating from 20 to 100 ºC. (a–c) Synchronous correlation spectra of **TD**. (d–f) Asynchronous correlation spectra of **TD**.

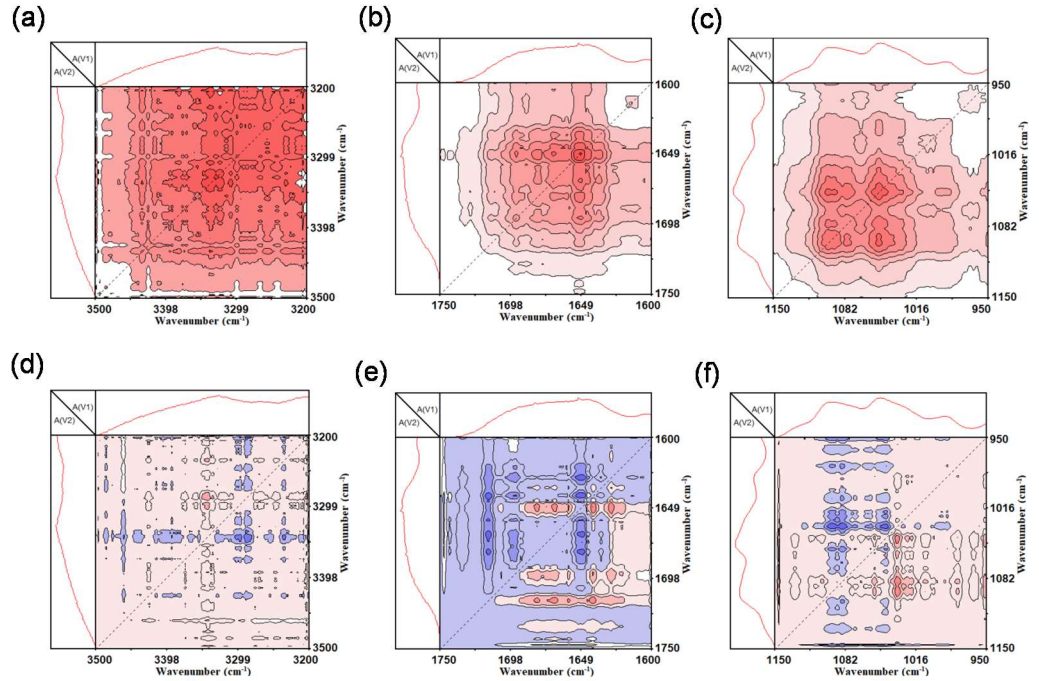

Figure S20. Synchronous and asynchronous correlation spectra of **UD** during heating from 20 to 100 ºC. (a–c) Synchronous correlation spectra of **UD**. (d–f) Asynchronous correlation spectra of **UD**.

12. Density Functional Theory (DFT) simulations

Table S7. Combination Gibbs free energy.

Compound 1	Ratio	Compound 2	Combination Gibbs free energy (kJ/mol)
T	1:1	**D**	-134.263
U	1:1	**D**	-129.159
T	1:1	**T**	-138.212
D	1:1	**D**	-168.258
U	1:1	**U**	-124.244

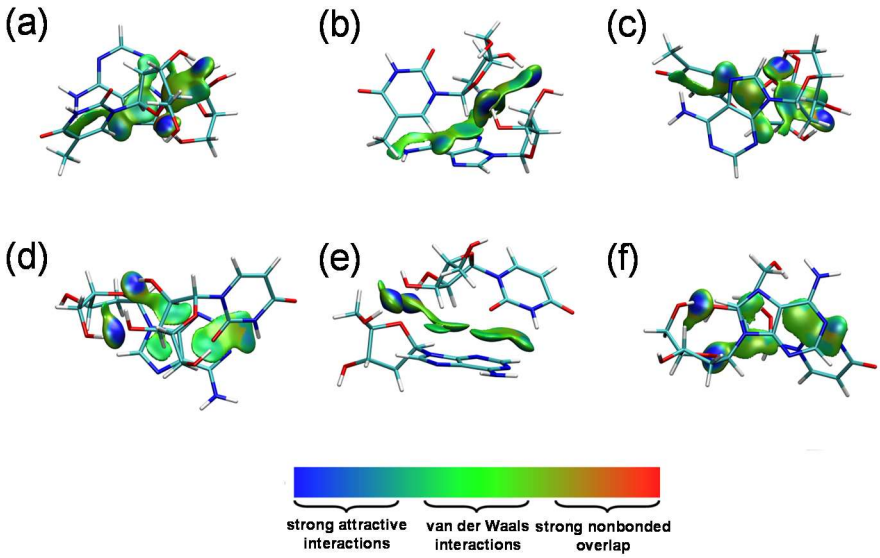

Figure S21. (a–c) The independent gradient model (IGM) isosurfaces for the interaction between **T** and **D** (molar ratio 1:1). (d–f) The IGM isosurfaces for the interaction between **U** and **D** (molar ratio 1:1). The color bar shows that blue, green, and red represent strong attraction interactions (hydrogen bonding), van der Waals interactions, and strong nonbonded overlap, respectively.

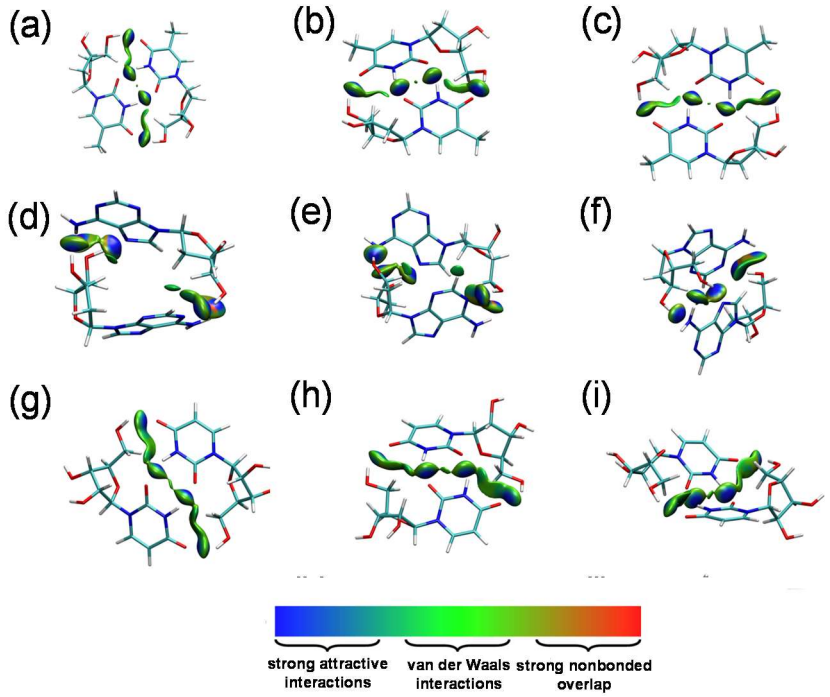

Figure S22. (a–c) The IGM isosurfaces for the interaction between **T** and **T** (molar ratio 1:1). (d–f) The IGM isosurfaces for the interaction between **D** and **D** (molar ratio 1:1). (g–i) The IGM isosurfaces for the interaction between **U** and **U** (molar ratio 1:1). The color bar shows that blue, green, and red represent strong attraction interactions (hydrogen bonding), van der Waals interactions, and strong nonbonded overlap, respectively.

13. Powder X-Ray Diffraction (PXRD) pattern of BSGs

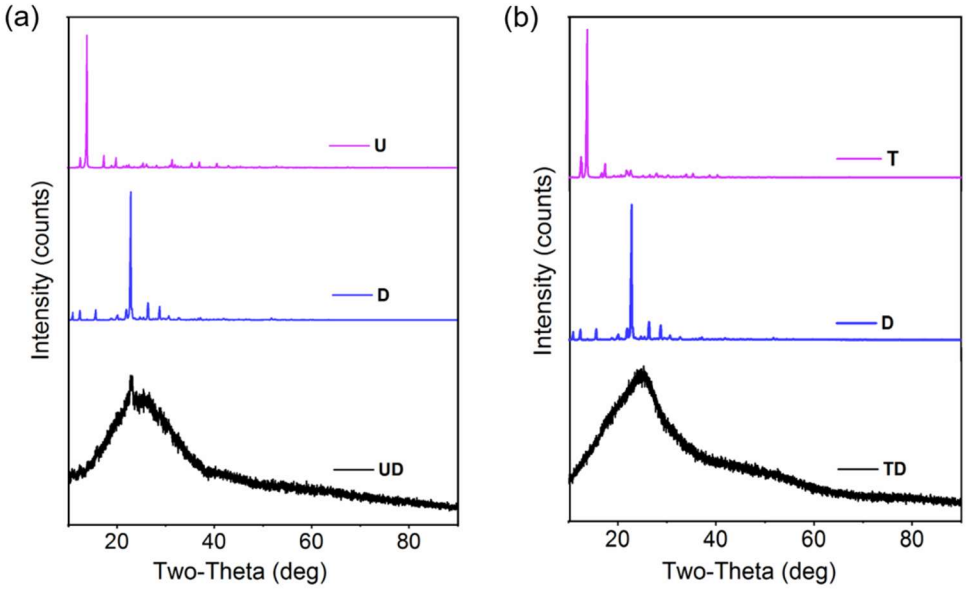

Figure S23. PXRD spectra of nucleosides and **BSG**s. (a) PXRD spectra of **T**, **D**, and **TD**. (b) PXRD spectra of **U**, **D**, and **UD**.

14. X-ray photoelectron spectroscopy (XPS) spectra of BSGs

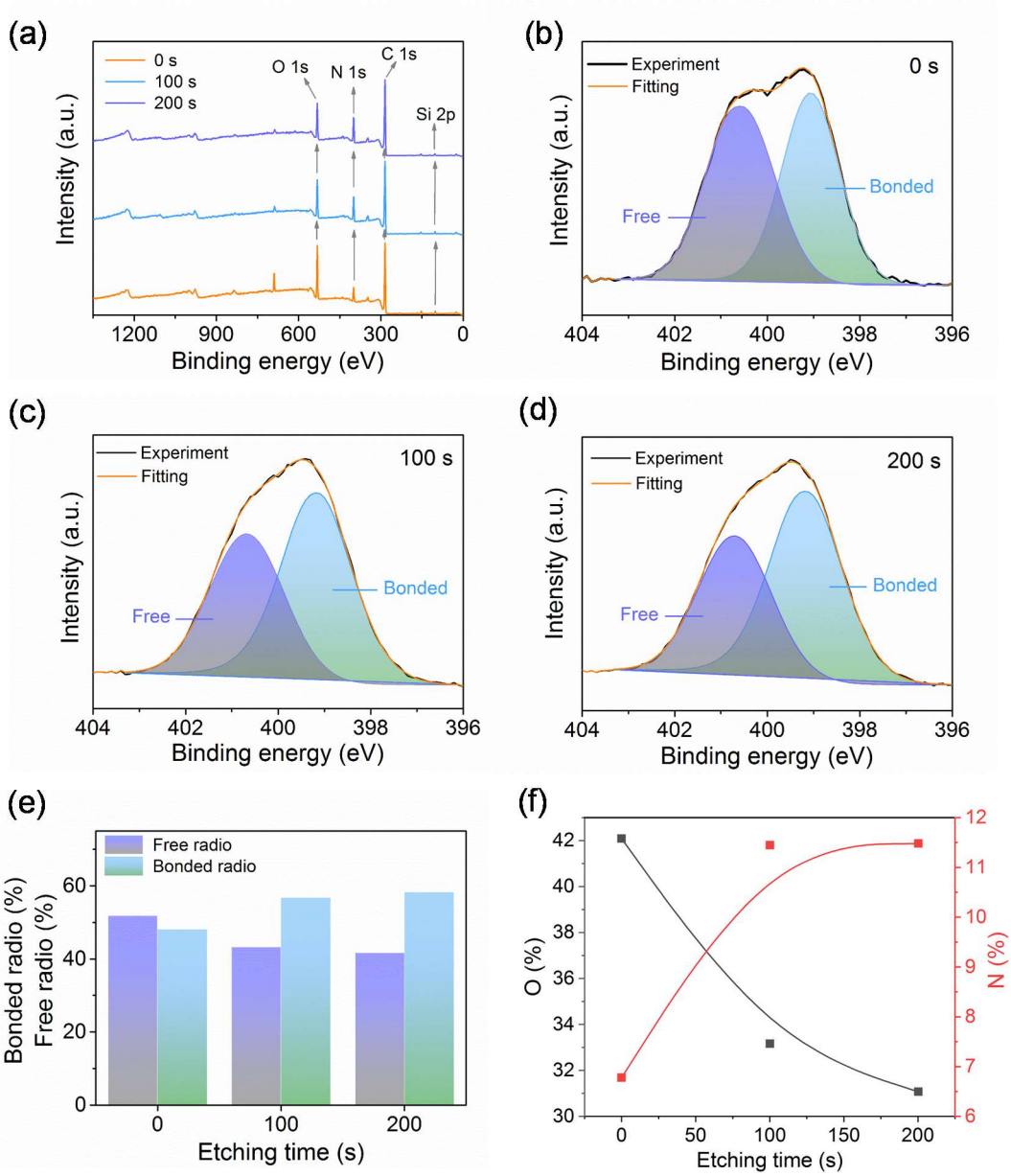

Figure S24. XPS spectra of **BSG**s. (a) Wide-scan XPS spectra of **UD** after different etching times, (b–d) Common and depth-dependent N 1s narrow scan for **UD**; (e) Percentage of "free" and "bonded" N-H motifs derived from N 1s narrow scan after different etching times. (f) Percentage of O 1s and N 1s narrow scan after different etching times.

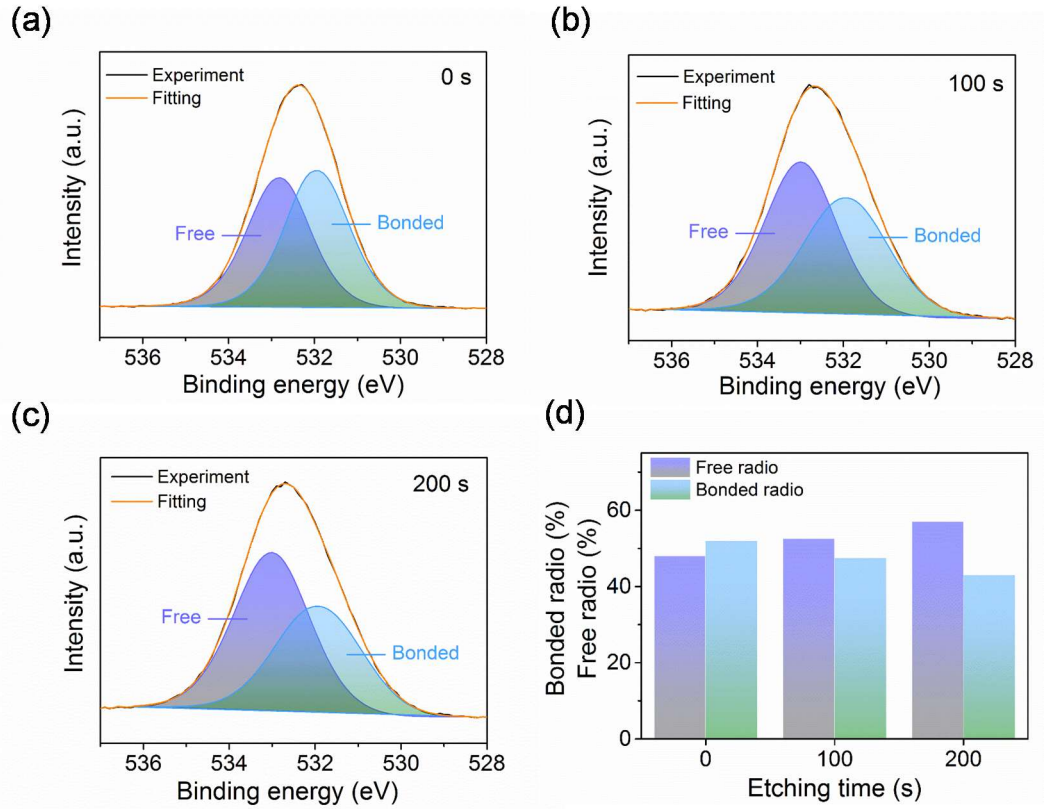

Figure S25. XPS spectra of **BSG**s. (a–c) Common and depth-dependent O 1s narrow scan for **UD**. (d) Percentage of "free" and "bonded" O-H motifs derived from O 1s narrow scan after different etching times.

15. Molecular dynamic (MD) simulations

Mechanical properties of BSGs

Table S8. Mechanical properties of **TD** at room temperature.

	Young modulus (GPa)		
	X	Y	Z
T+D	6.98	4.57	5.80
T+D+1H_2O	6.70	5.37	5.79
T+D+3H_2O	6.72	4.97	5.41
T+D+10H_2O	6.66	4.82	5.35

Table S9. Mechanical properties of **UD** at room temperature.

	Young modulus (GPa)		
	X	Y	Z
U+**D**	7.68	7.84	8.02
U+**D**+1H_2O	7.86	6.98	7.48
U+**D**+3H_2O	7.84	6.63	7.24
U+**D**+10H_2O	8.46	6.63	5.54

Fraction of free volume (FFV) of BSGs

$FFV = V_f/V_{sp} = (V_{sp}-1.3V_w)/V_{sp}$

Where V_{sp} is the cell volume. V_w is the van der Waals volume obtained from the van der Waals surface. V_f is free volume.

Table S10. *FFV* of **TD** at room temperature.

	Volume (Å^3)	Occupied volume (Å^3)	Free volume (Å^3)	*FFV* (%)
T+**D**	29731.22	27030.9	2700.32	9.08
T+**D**+1H_2O	30220.59	27384.45	2836.14	9.38
T+**D**+3H_2O	31079.51	28062.51	3017	9.71
T+**D**+10H_2O	34060.76	30739.21	3321.55	9.75

Table S11. *FFV* of **UD** at room temperature.

	Volume (Å^3)	Occupied volume (Å^3)	Free volume (Å^3)	*FFV* (%)
U+**D**	28512.42	26098.85	2413.57	8.46
U+**D**+1H_2O	28875.87	26545.82	2330.05	8.07
U+**D**+3H_2O	29710.9	27097.82	2613.08	8.80
U+**D**+10H_2O	32808.16	29916.02	2892.14	8.82

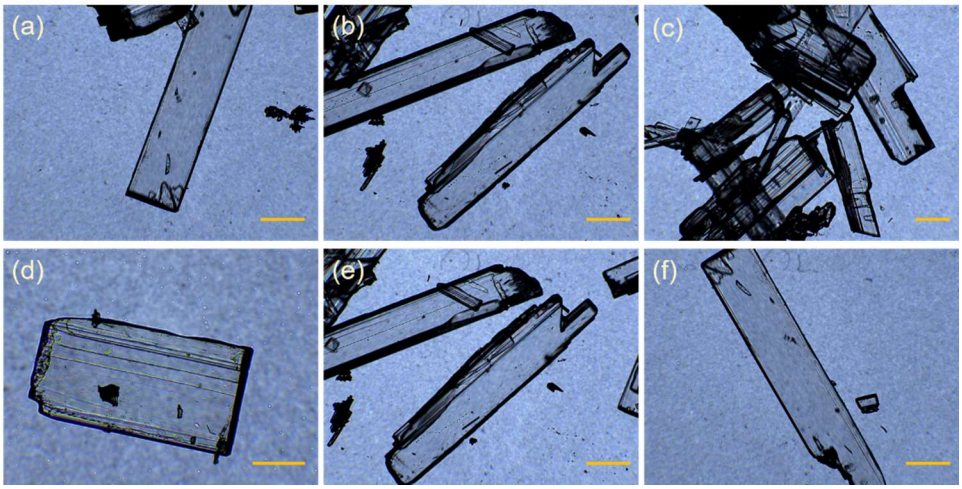

Figure S26. Optical microscope images of single crystal **T**. Scale bar represents 5 μm.